

Classification of the factors causing the change of the optical fiber strain by using the Brillouin reflectograms

I V Bogachkov

Omsk State Technical University, 11, Mira ave., Omsk, 644050, Russia

Abstract. A classification of the factors causing the change of the optical fiber strain by using the Brillouin reflectograms is considered.

The differences of Brillouin reflectograms with strain along the optical waveguide are discussed under various impacts: temperature and mechanical longitudinal stretching.

Reference Brillouin reflectograms for different kinds of optical fibers from the database are capable of improving a process of classification of potentially hazardous sections (sections of optical fibers with high mechanical strain or changed temperature) in the optical fiber.

The results presented in this paper allow us on the basis of the analysis of Brillouin multi-reflectograms to identify a factor that has a predominant impact on the fiber strain in the investigated sections of the optical fibers in fiber optical communication lines.

Keywords. Optical fiber, strain, temperature, Mandelstam – Brillouin scattering, backscattered signal, Brillouin frequency shift.

1. Introduction

Comprehensive development, high-quality and failure-free service of fiber optical communication lines (FOCLs) require improvement of monitoring systems and early diagnostics for troubleshooting of faults and potentially hazardous sections in the optical fibers (OFs).

Early diagnostics is an early detection of the OF sections located in the laid optical cables (OCs), which over time can lead to the breakdown of the OF and disfunction of the fiber optical transmission system [1 – 5].

The potentially hazardous (“bad”) sections are OF sections with high mechanical strain and modified temperature, etc. The high strain of the OF (more than 0.2 % according to the “Fujikura” Ltd and “Corning”) in the laid OCs impacts the durability of a FOCL. At this strain it decreases to 5 years instead of the expected 25 years, and at a strain of about 1 % is less than a year [1, 3, 4].

Temperature transformations in OF can signal the appearance of the “bad” fiber sections on the cable routing (a breakthrough heating duct, cracks in protective structures, an unauthorized access to fibers, etc.) [5 – 7].

Therefore, it is necessary to monitor the physical state of the OFs in the monitoring system for the FOCL, in particular, mechanical strain.

For early diagnostics of optical fibers (OFs) located in the laid optical cables (OCs) the specialized devices – Brillouin optical time-domain reflectometers (BOTDRs) can be used [1 – 7]. The BOTDR allows us to troubleshoot the OF sections with high longitudinal strain and modified temperature.

The standard optical time-domain reflectometers (OTDR) widely applied in monitoring systems for OFs analyze a Rayleigh scattering, and can't solve such tasks.



The Raman reflectometers are used for detection only of temperature transformations, and they analyze the Mandelstam – Landsberg (or Raman) backscatter spectrum.

Backscattered signal containing components of the Mandelstam – Brillouin scattering (MBS) is analyzed in the BOTDR [1 – 4].

Getting the distribution pattern of the Mandelstam – Brillouin backscatter spectrum (MBBS) along the OF (3D-BOTDR reflectogram of the MBBS distribution) the Brillouin frequency shift (f_B) is determined.

As a result, the pattern of strain distribution along the optical waveguide is achieved [1 – 7].

After the determination of f_B and OF strain, there is uncertainty in the identification of the factors causing change in f_B in the tested section, since the f_B depends on both the longitudinal strain of the OF [1 – 4] and the OF temperature [5 – 10]. Despite the fact that the potentially “bad” section of a FOCL is clearly appeared due to the major changes in f_B and OF strain, it is desirable to classify which factors (longitudinal strain of the OF or temperature transformation) is predominant.

2. The theory

The MBBS profile along the optical waveguide is defined by separating the difference between the radiation frequency of the probe laser of f_L and the spectrum frequencies of the backscattered signal in the receive path. The difference frequencies (corresponding to MBBS) have a band from 9.9 GHz to 11.9 GHz at the wavelength of the probe laser (λ_L) of 1.55 μm of the emitting laser.

The key feature of the BOTDR (compared with other devices for determining the strain in an OF, for example, the Brillouin optical time-domain analysis (BOTDA)) is one-end access to the OF.

The relationship of the MBBS peak shift of Δf_B and the intensity of the anti-Stokes wave of ΔI with transformations in Young's module (strain) of ΔE_ε and temperature of ΔT can be given by matrix form:

$$\begin{bmatrix} \Delta f_B (\Delta E_\varepsilon, \Delta T) \\ \Delta I (\Delta E_\varepsilon, \Delta T) \end{bmatrix} = \begin{bmatrix} C_f^\varepsilon & C_f^T \\ C_I^\varepsilon & C_I^T \end{bmatrix} \begin{bmatrix} \Delta E_\varepsilon \\ \Delta T \end{bmatrix}, \quad (1)$$

where C_f^ε , C_f^T , C_I^ε and C_I^T are coupling coefficients for the corresponding parameters.

Typical values of these coefficients for G.652 OF under normal conditions (at room temperature and without longitudinal strain) are as follows: $C_f^\varepsilon = 48 \text{ kHz}/\mu\varepsilon = 480 \text{ MHz}/\%$, $C_f^T = 1.06 \text{ MHz}/^\circ\text{C}$ (values related to a ΔI), $C_I^\varepsilon = -8.07 \cdot 10^{-6}/\mu\varepsilon = -0.0807/\%$, $C_I^T = 0.0033/^\circ\text{C}$ [10].

These coefficients are not mutually independent.

There are other values and interpretations of these coefficients [8 – 9].

Obtaining the distribution pattern of the MBBS, the coefficients of Δf_B and of ΔI are determined, after which it is necessary to invert the matrix to find the ΔE_ε and ΔT .

$$\begin{bmatrix} \Delta E_\varepsilon (\Delta f_B, \Delta I) \\ \Delta T (\Delta f_B, \Delta I) \end{bmatrix} = \frac{1}{C_f^\varepsilon C_I^T - C_I^\varepsilon C_f^T} \begin{bmatrix} C_I^\varepsilon & -C_f^T \\ -C_I^T & C_f^\varepsilon \end{bmatrix} \begin{bmatrix} \Delta f_B \\ \Delta I \end{bmatrix}. \quad (2)$$

Brillouin frequency shift (f_B) is related to the features of the propagation medium by the following equation:

$$f_B(E_\varepsilon, T) = 2f_L v_{Aef}(E_\varepsilon, T) n_{ef} / c = 2v_{Aef}(E_\varepsilon, T) n_{ef} / \lambda_L. \quad (3)$$

where $v_{Aef}(E_\varepsilon, T)$ is the velocity of a hyperacoustic wave depending on the temperature, strain and core structure; n_{ef} is the effective refractive index of the medium, c is the velocity of light in vacuum [4 – 7].

The relationship is also expressed by

$$f_B(E_\varepsilon, T) = f_{B0} + C_f^\varepsilon (E_\varepsilon - E_0) + C_f^T (T - T_0), \quad (4)$$

where “0” are indexes corresponding to normal conditions (at room temperature and without longitudinal stretching force) [4 – 6].

Probing the OF by short pulses the distribution of MBBS along the optical waveguide is determined. After the analysis of the distribution pattern of the MBBS in the OF the $f_B(E_\rho, T)$ (values of MBBS peaks) are found along the OF, which then allows us to determine the degree of strain of all OF sections and to troubleshoot the distributed irregularities.

Analyzing f_B by Brillouin reflectograms, there is uncertainty in the identification of the factors causing change in f_B in the tested section, since the f_B depends on both the longitudinal strain of the OF and the OF temperature [1 – 7].

Therefore, the detection of the factor causing the shift of f_B in the tested OF is useful for early OF diagnostics. This allows us to estimate the real danger degree of the factor (short-time and long-time) for OF of the FOCL.

3. Analysis of experimental Brillouin reflectograms under various impacts

We analyze the impact of various disturbing factors on Brillouin reflectograms.

Fig. 1 – Fig. 3 show the multi-reflectograms of BOTDR with a major longitudinal stretching force on the OF. Each multi-reflectogram presents the dependence of the fiber strain (“Strain”) along the optical waveguide, the MBBS profile (“Brillouin Spectrum”), the width of the MBBS (“B. S. Width”) and the level of the backscattered signal (“Loss”) [3, 4].

Fig. 1 shows a multi-reflectogram of the BOTDR with irregular impact of a longitudinal force of 6 N on the OF [4].

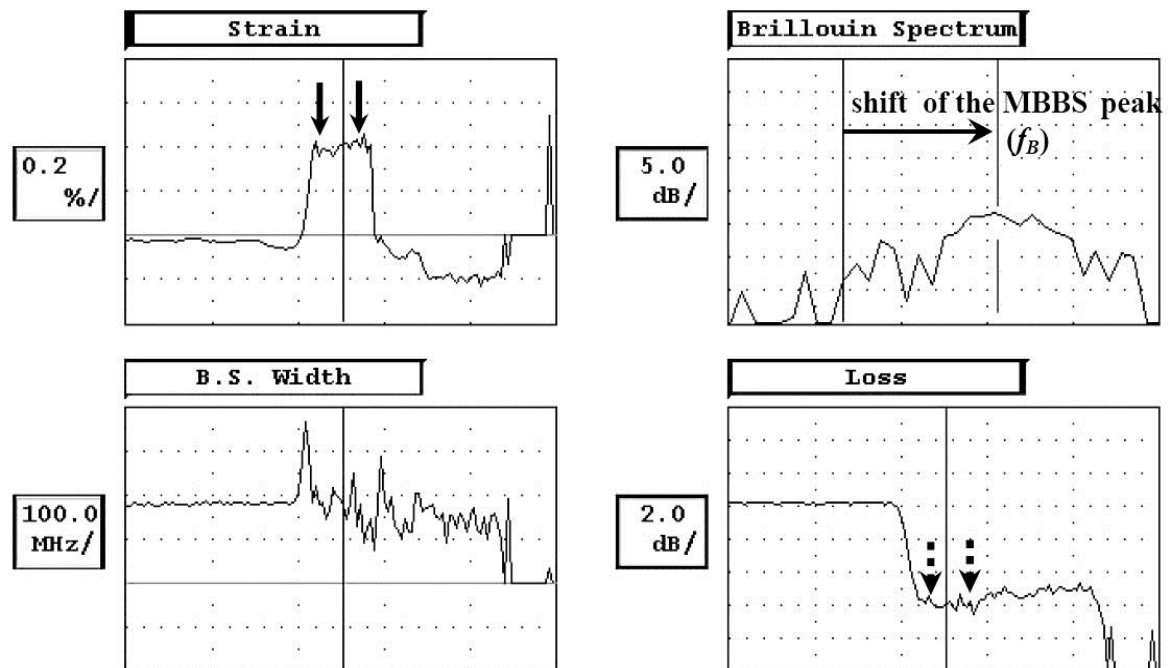


Figure 1. Multi-reflectogram along the G.652 optical waveguide with irregular longitudinal stretching force of sections of 6 N.

Transformations in the strain graph (marked by solid arrows) have been discussed [4]. It is important to note that a decrease in the intensity of the backscattered MBS signal (marked by dashed arrows) is observed in the loss graph.

Fig. 2 shows a similar multi-reflectogram of BOTDR with uniform impact of the same longitudinal stretching force (6 N) on the OF.

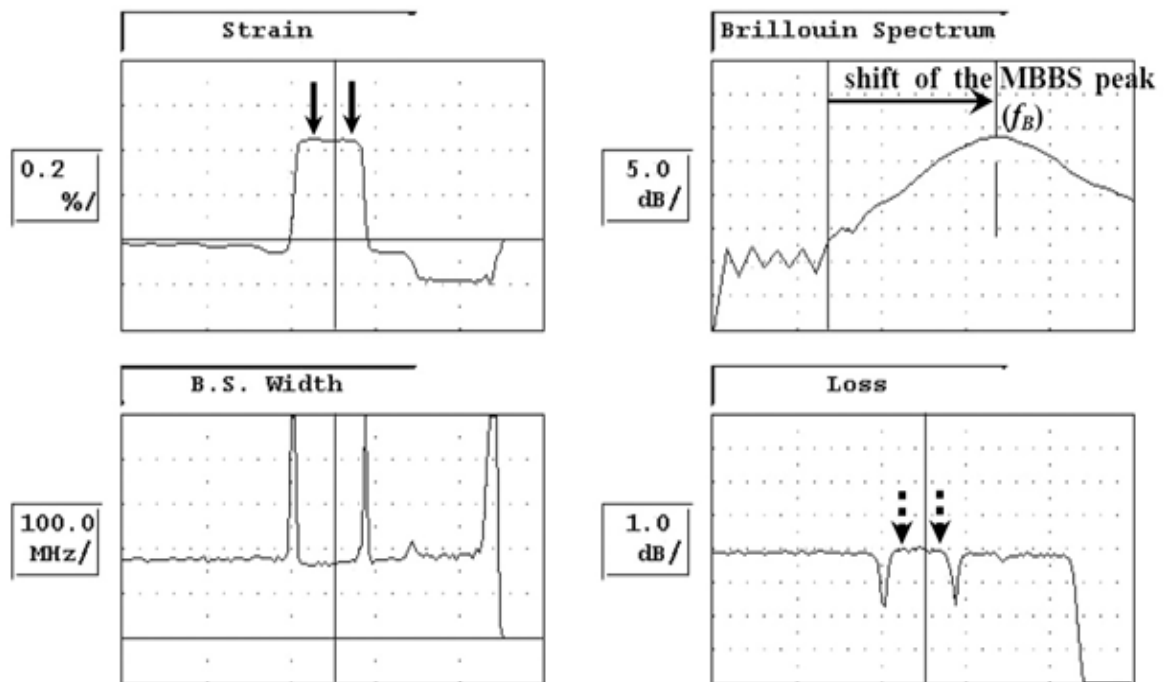


Figure 2. Multi-reflectogram along the G.652 optical waveguide with uniform longitudinal stretching force of sections of 6 N.

Transformations are significantly clearer in the strain graph [4], while the intensity of the backscattered MBS signal is almost constant (index of C_l^f is not very different from zero) in the loss graph.

Fig. 3 shows a multi-reflectogram of BOTDR with uniform impact of the longitudinal stretching force of more than 10 N on the OF [4].

The intensity of the backscattered MBS signal decreases slightly (by about 0.3 dB, which corresponds to the value) at the strained section in the loss graph with noticeable transformations in the strain graph (more than 1 % [4]).

Thus, either the decrease in intensity or nonincreasing graph (ideally) is observed in the intensity graphs of the backscattered MBBS signal at the longitudinal strain of the OF in all experiments [1 – 4].

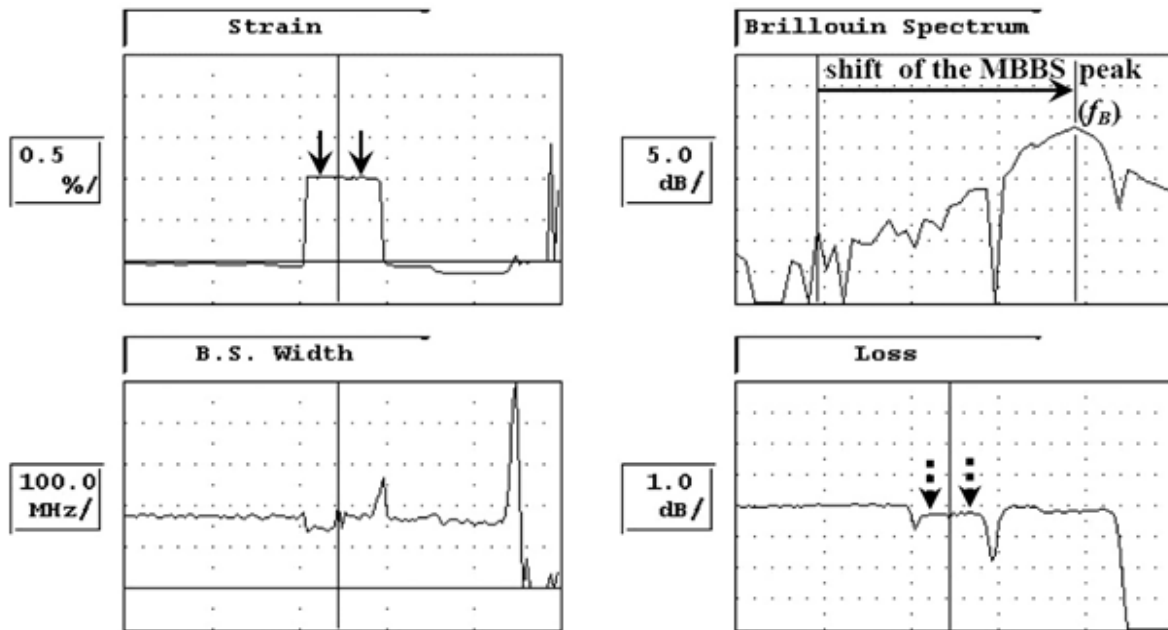


Figure 3. Multi-reflectogram along the G.652 optical waveguide with longitudinal stretching force of sections of more than 10 N.

Moreover, a noticeable decrease in the intensity of the backscattered MBBS signal is observed even with small transverse impacts due to the irregular stretching force.

For comparison, Fig. 4 and Fig. 5 show the multi-reflectograms of the BOTDR with temperature impacts on the optical waveguide [5 – 7] composed of different kinds of optical fibers: G.652+LBL+LEAF+ULTRA (apart from the usual OF of the normalizing coil, the G.652 OF “Corning”: LBL and ULTRA – OF with improved bending features, as well as G.655 OF “Corning” – LEAF – OF with a non-zero dispersion-shifted fiber are used) [12].

Fig. 4 shows the multi-reflectograms of the BOTDR with heated OF sections to +90°C.

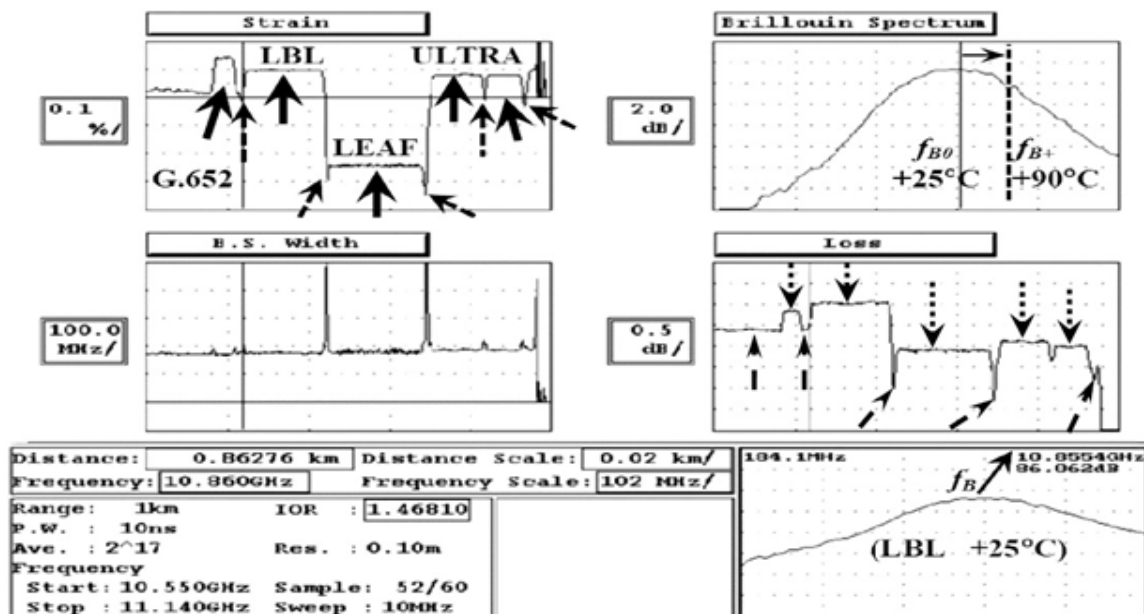


Figure 4. Multi-reflectogram along the optical waveguide with heated sections to +90°C.

Transformations in the strain graph (marked by solid thick arrows) have been discussed earlier [12]. It should be noted that a noticeable increase in the intensity of the backscattered MBS signal (marked by dot-and-dash arrows) is seen in the loss graph. Sections with room temperature are shown by thin dashed arrows.

At room temperature, in addition to a rise of level at the initial section of the erbium-doped fiber (EDF) [1, 12], an increase in the intensity of the backscattered MBS signal can be observed only at the obvious reflective events such as a fiber breakage.

Fig. 5 presents a similar multi-reflectogram with cooled sections of the same optical waveguide to -15°C [12].

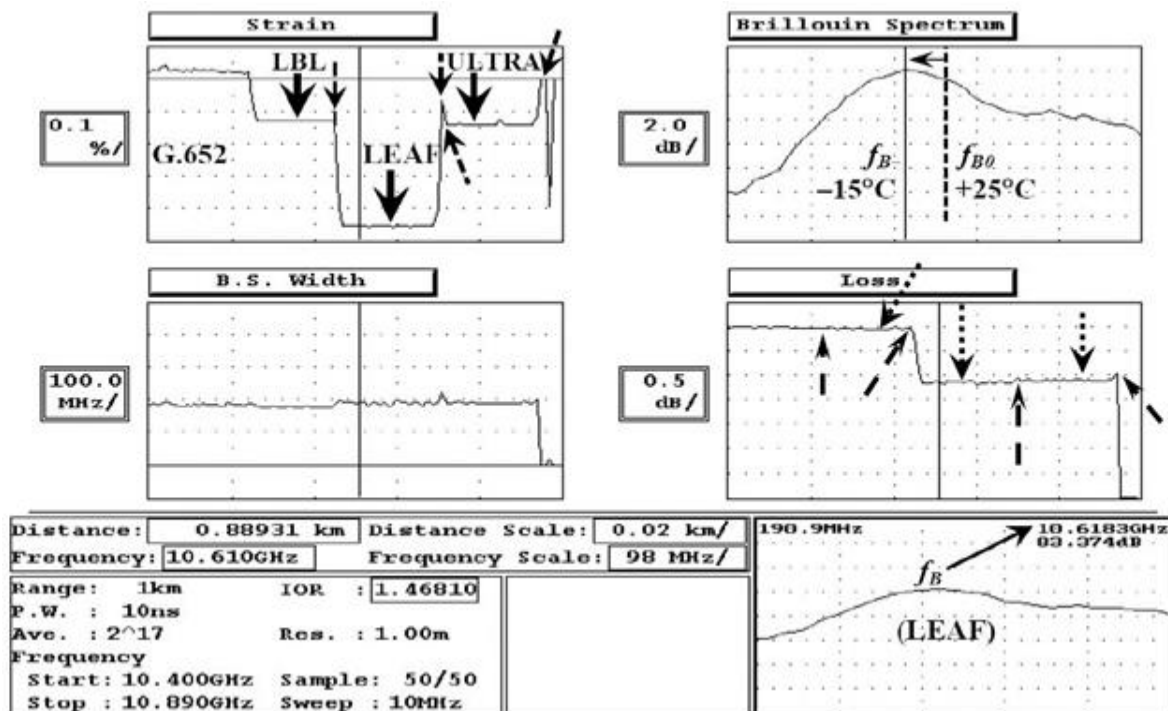


Figure 5. Multi-reflectogram along the optical waveguide with cooled sections to -15°C .

The intensity of the backscattered MBS signal decreases slightly in the loss graph with noticeable strain transformations in the cooled sections.

The results of all tests with temperature transformations for different kinds of OFs [12] are summarized in table 1.

Table 1.

| Test feature | | G.652 | | LBL | | LEAF | | ULTRA | |
|----------------|-------|-------|-------|-------|-------|-------|-------|-------|-------|
| | | f_B | A, dB |
| f_{B0} , GHz | +25°C | 10.87 | 85.79 | 10.84 | 86.20 | 10.66 | 83.80 | 10.83 | 84.20 |
| f_{B-} , GHz | -12°C | 10.86 | 85.29 | 10.79 | 85.76 | 10.62 | 83.40 | 10.78 | 83.84 |
| f_{B+} , GHz | +50°C | 10.89 | 86.11 | 10.87 | 86.44 | 10.69 | 84.14 | 10.86 | 84.51 |
| | +60°C | 10.90 | 86.31 | 10.88 | 86.55 | 10.70 | 84.27 | 10.87 | 84.63 |
| | +75°C | 10.92 | 86.51 | 10.90 | 86.75 | 10.72 | 84.57 | 10.89 | 84.87 |
| | +90°C | 10.94 | 86.66 | 10.91 | 87.02 | 10.73 | 84.74 | 10.90 | 85.16 |

Fig. 6 shows the final intensity dependences of the backscattered signal on the temperature $A(T)$ for different kinds of OFs.

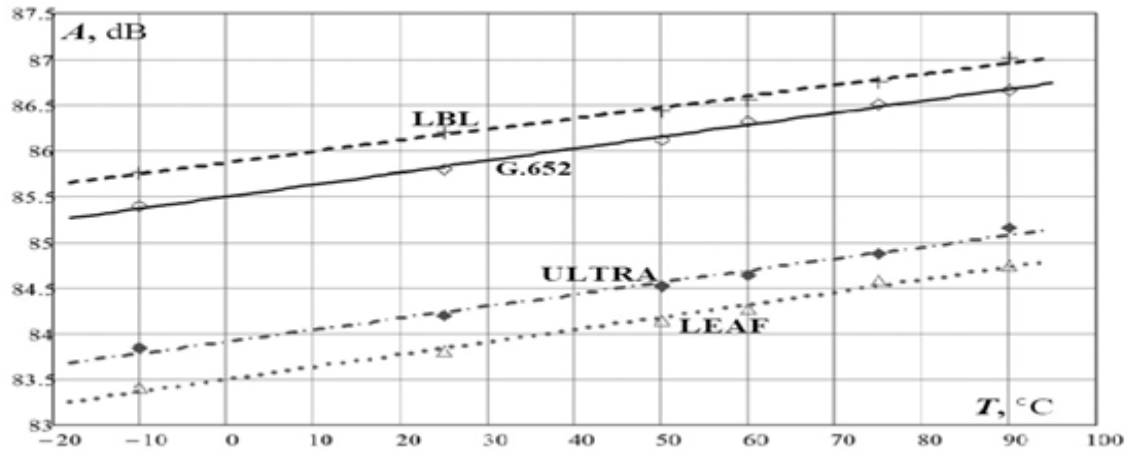


Figure 6. Dependence of intensity of a backscattered signal on temperature.

The results suggest that transformations in the intensity of the backscattered MBS signal are equal to $+0.013 \text{ dB}/^\circ\text{C}$ with an increase in temperature in the tested range. A greater temperature stability and an accuracy of test in the temperature range from $+50^\circ\text{C}$ to $+90^\circ\text{C}$ were achieved, and these transformations were in the range of $+0.014 \dots +0.015 \text{ dB}/^\circ\text{C}$ for different kinds of the OFs.

Attempts to identify the temperature impacts on the final Brillouin reflectogram have already been made on the basis of the analysis of Rayleigh multi-reflectogram [2].

According to works [2, 10, 12–14] the $C_f^T = 0.0033/^\circ\text{C}$ which corresponds to increase in the power of the backscattered MBS signal of $1.0033/^\circ\text{C}$, so the value of $+0.0145 \text{ dB}/^\circ\text{C}$ is achieved.

The analysis of the multi-reflectograms obtained in other tests [5–7] with temperature transformations from -20°C to $+250^\circ\text{C}$ also have showed a similar increase in the intensity of the backscattered MBS signal with an temperature increase.

Thus, the obtained dependences allow us to distinguish the temperature change:

$$P(T) = P(T_0) + 1.0033(T - T_0) = P_0 + 1.0033\Delta T \quad \text{or}$$

$$P(T)[\text{dB}] = P(T_0)[\text{dB}] + 1.0145[\text{dB}/^\circ\text{C}]\Delta T, \quad (5)$$

$$\Delta T = T - T_0 = \frac{P(T)/P(T_0)}{1.0033} = \frac{P(T)[\text{dB}] - P(T_0)[\text{dB}]}{1.0145[\text{dB}/^\circ\text{C}]} \quad (6)$$

From (6) it is possible to determine the change of f_B and fiber strain (E_ε) at the fixed temperature:

$$f_B(E_\varepsilon) = f_{B0} + C_f^\varepsilon(E_\varepsilon - E_{\varepsilon0}) + f_{BT}, \quad (7)$$

where $f_{BT}(T) = f_{B0} + C_f^T(T - T_0)$ – Brillouin frequency shift, caused precisely only temperature;

$$E_\varepsilon = E_{\varepsilon0} + \frac{f_B - f_{B0} - f_{BT}}{C_f^\varepsilon} \quad (8)$$

4. Conclusion

The obtained results enable us to identify a factor that has a predominant impact on the OF strain in the investigated sections of the OF in the FOCL by using the analysis of Brillouin multi-reflectograms. It can increase the efficiency of early diagnostics of “bad” sections of the OFs in the FOCL.

We can improve a velocity and an efficiency of tests by using the f_{B0} from an OF database of different kinds and companies.

If the transformation in the intensity of the backscattered MBS signal is also observed in addition to the change in f_B , it is possible to classify which factor causes the change of f_B : transformation of temperature or longitudinal stretching force.

5. Acknowledgments

The work was performed with the financial support of the Ministry of Education and Science of the Russian Federation within the scope of the base part of a State Assignment within the sphere of scientific activity (Project No. 8.9334.2017/8.9).

References

- [1] Bogachkov I V 2018 Determination of mechanical stressed places of optical fibers in optical cables using Brillouin reflectometers *T-comm* **12**, **12** pp 78–83 DOI 10.24411/2072-8735-2018-10205
- [2] Viavi MTS/T-BERD 8000 – fiber sensing module DTSS module: user manual *Viavi Solutions* 94 p.
- [3] Bogachkov I V 2016 Experimental Researches of the Brillouin Backscatter Spectrum in Optical Fibers at Influence of the Essential Stretching Forces *Dynamics of Systems, Mechanisms and Machines (Dynamics-2016): proceedings* pp 1–6 DOI: 10.1109/Dynamics.2016.7818985
- [4] Bogachkov I V and Gorlov N I 2016 Investigation of effects of longitudinal stretching of optical fibers on Brillouin backscattering spectrum *International Conference on Actual Problems of Electronic Instrument Engineering (APEIE–2016): proceedings* **1**, **1** pp 162–168 DOI: 10.1109/APEIE.2016.7802243
- [5] Bogachkov I V 2016 Experimental Researches of Temperature Dependences of Brillouin Backscatter Spectrum in Optical Fibers of Various Types *Dynamics of Systems, Mechanisms and Machines (Dynamics-2016): proceedings* pp 1–7 DOI: 10.1109/Dynamics.2016.7818987
- [6] Bogachkov I V 2017 Temperature Dependences of Mandelstam – Brillouin Backscatter Spectrum in Optical Fibers of Various Types *Systems of Signal Synchronization, Generating and Processing in Telecommunications (SINKHROINFO–2017): proceedings* pp 1–6 DOI: 10.1109/SINKHROINFO.2017.7997505
- [7] Bogachkov I V and Gorlov N I 2016 Researches of the influence of temperature changes in optical fibers on the Brillouin backscattering spectrum *International Conference on Actual Problems of Electronic Instrument Engineering (APEIE–2016): proceedings* **1**, **1** pp 157–161 DOI: 10.1109/APEIE.2016.7802241
- [8] Horiguchi T, Kurashima T and Koyamada Y 1992 Measurement of temperature and strain distribution by Brillouin frequency shift in silica optical fibers *Distributed and Multiplexed Fiber Optic Sensors* **1797** pp 2–13
- [9] Parker T, Farhadiroushan M, Handerek V and Rogers A 1997 Temperature and strain dependence of the power level and frequency of spontaneous Brillouin scattering in optical fibers *Optics letters* **26**, **11** pp 787–789
- [10] Belal M and Newson T P 2012 Experimental examination of the variation of the spontaneous Brillouin power and frequency coefficients under the combined influence of temperature and strain *Journal of Lightwave Technology* **30**, **8** pp 1250–1255
- [11] Bao X and Chen L 2011 Recent Progress in Brillouin Scattering Based Fiber Sensors *Sensors* **11** pp 4152–4187
- [12] Bogachkov I V 2019 Research of the features of Mandelstam – Brillouin backscattering in optical fibers of various types *T-comm* **13**, **1** pp 60–65 DOI 10.24411/2072-8735-2018-10292
- [13] Zou W, Long X. and Chen J. 2015 Brillouin Scattering in Optical Fibers and Its Application to Distributed Sensors *Intech: Advances in Optical Fiber Technology: Fundamental Optical Phenomena and Applications* pp 1–53 DOI:10.5772/59145
- [14] Bogachkov I V 2019 Improved data processing algorithms in Brillouin reflectometers for determining the strain of optical fibers *T-comm* **13**, **7** pp 60–64 DOI 10.24411/2072-8735-2018-10292